RAPID COMMUNICATIONS

PHYSICAL REVIEW B VOLUME 37, NUMBER 4 1 FEBRUARY 1988

Flux quantization in periodic networks containing tiles with irrational ratio of areas

P. Santhanam, C. C. Chi, and W. W. Molzen
IBM Thomas J. Watson Research Center, P.O. Box 218, Yorktown Heights, New York 10598
(Received 28 August 1987)

We report measurements of the superconducting-normal transition boundary $T_c(H)$ of two-dimensional periodic networks with two different space-group symmetries in a magnetic field. Each network is a mixture of squares and equilateral triangles. In both cases, we observe maxima in $T_c(H)$ with *one major period,* which does not correspond to the area of either the square or the triangle. We interpret the results in terms of flux configurations whose energies are sensitive to the geometry of a given network.

The study of phase transitions in two-dimensional (2D) systems[1] is an exciting branch of condensed-matter physics. Substantial work has been done to understand the superconducting-to-normal transition in periodic arrays of Josephson junctions[2] and proximity-effect-coupled superconducting islands.[3] These systems display a wide variety of phenomena that include Kosterlitz-Thouless vortex-antivortex unbinding transition[1] in zero magnetic field and periodic oscillations in the resistance as a function of an external magnetic field.

Superconducting wire networks[4-6] near the transition are simpler to understand compared to the junction arrays. The transition temperature $T_c(H)$ of a periodic lattice[4] (square, triangular, or honeycomb) exhibits oscillations as a function of a magnetic field, with a fundamental period corresponding to a flux quantum, Φ_0 ($=hc/2e=20.7\ \mu m^2 G$), in the unit cell. In addition, there are other fine structures at rational fractions p/q of this basic period, representing the commensurability of the flux lattice with the underlying geometrical lattice. Arbitrary values of the magnetic field result in frustration of the flux lattices. Mean-field calculations[7-9] based on linearized Ginzburg-Landau (GL) theory have been enormously successful in explaining the details of the experimentally observed behavior. Notably, the GL equation for the order parameter at the nodes of a network has been mapped[7] onto the Bloch equation for electrons in the 2D tight-binding model for the same lattice geometry. Thus, the superconducting-normal phase boundary is related to the band edge of the corresponding Bloch spectrum. The results of Pannetier *et al.*[4] on periodic lattices, along with the conclusions of the recent experiments in fractal[5] and quasicrystalline[6] networks, clearly demonstrate that the behavior of $T_c(H)$ reflects the properties of the lattice under consideration.

The periodic networks studied until now have mostly corresponded to simple two-dimensional Bravais lattices. The primary objective of this study is to see the effect of two different tiles with an irrational ratio of areas in a periodic lattice. Secondly, we like to study the influence of the exact geometry on $T_c(H)$ and other transport properties of different periodic lattices with the same numbers and the same kinds of tiles.

The samples were prepared using submicrometer electron-beam lithography.[10] Each network is a periodic mixture of equilateral triangles and squares. The wire defining the network is nominally 300-Å-thick aluminum of width 0.5 μm. The distance a_0 between any two adjacent nodes is 2.4 μm and the size of the network is $720\times720\ \mu m^2$. Two opposite edges of an array are shorted by a 25-μm-wide strip for making current and voltage contacts. The first network [shown in Fig. 1(a)] has the symmetry[11] corresponding to the two-dimensional space group $P4gm$. The second network [shown in Fig. 1(b)] corresponds to the two-dimensional space group[11] $C2mm$ with a centered rectangular Bravais lattice.

For periodic lattices with tiles of two different areas, one would expect the locations of the maxima in $T_c(H)$ to correspond to either of the areas and/or the sum of the areas. However, as the analysis and the experimental data below indicate, there is only one major period that does *not* correspond to the area of either the square or the triangle.

The measurement of $T_c(H)$ is done similar to the other experiments[4-6] with a bias current of 10 μA. The typical sample resistance was 2 Ω at 4.2 K, and T_c for various samples ranged from 1.35 to 1.55 K. We show in Fig. 2 the $T_c(H)$ behavior of the two networks, for both positive and negative fields up to $\simeq$20 G. We have already subtracted the background proportional to H^2 due to the flux penetration in the wires of finite width. The magnetic field corresponding to a superconducting flux quantum in

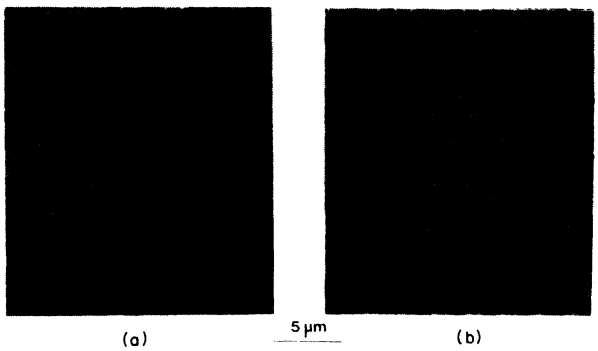

FIG. 1. Electron micrographs of samples. (a) $P4gm$ symmetry. (b) $C2mm$ symmetry.

the square is 3.59 G and that in the triangle is 8.30 G. Now we discuss some major features of Fig. 2. In both networks, the maxima in T_c occur with a characteristic period of $H_p \simeq 1.96$ G. We can write the locations of the peaks as corresponding to n times the basic field H_p, where n is an integer or certain rational fractions. The large peaks in $T_c(H)$ corresponding to $n=4$, 5, and 9 are observed in both networks. The relative magnitudes of the various other peaks are different for the two geometries. In the $C2mm$ case [Fig. 2(b)], the structures at $n=1$, 2, 6, 7, and 8 are less prominent compared to the $P4gm$ geometry, but they can be clearly seen in the second derivatives. There are additional maxima in Fig. 2(b), corresponding to $n=\frac{5}{3}$ and $n=\frac{22}{3}$. The peak at $n=\frac{9}{2}$ is larger than for the $P4gm$ case. Our analysis below addresses these features.

In the following discussion, we shall identify the flux configurations that lead to the experimentally observed structures using an intuitive approach.[6] If N_{sq} (N_{tr}) is the total number of squares (triangles) in the array and n_{sq} (n_{tr}) is the average flux in each square (triangle) in units of Φ_0, the average magnetic field over the array is given by

$$H_{av}=\Phi_0\left(\frac{N_{sq}n_{sq}+N_{tr}n_{tr}}{N_{sq}A_{sq}+N_{tr}A_{tr}}\right), \tag{1}$$

where A_{sq} (A_{tr}) is the area of the square (triangle). $A_{tr}=(\sqrt{3}/4)A_{sq}$ and $N_{tr}=2N_{sq}$ and therefore Eq. (1) reduces to

$$H_{av}=H_{sq}\left(\frac{n_{sq}+2n_{tr}}{1+\sqrt{3}/2}\right)\equiv H_p n\,, \tag{2}$$

where H_{sq} ($=\Phi_0/A_{sq}$) is the field corresponding to a flux quantum in the square, $n=n_{sq}+2n_{tr}$ and $H_p=H_{sq}/(1+\sqrt{3}/2)$. For our samples, H_p is 1.93 G and thus corresponds to the basic period discussed above. One expects (in general) the maxima in T_c to correspond to integral values of n_{sq} and n_{tr}. In fact, similar to the simple Bravais lattices, there may be local maxima in T_c for $n_{sq}=p/q$ (a rational fraction), corresponding to p flux quanta in q squares and similarly for n_{tr}.

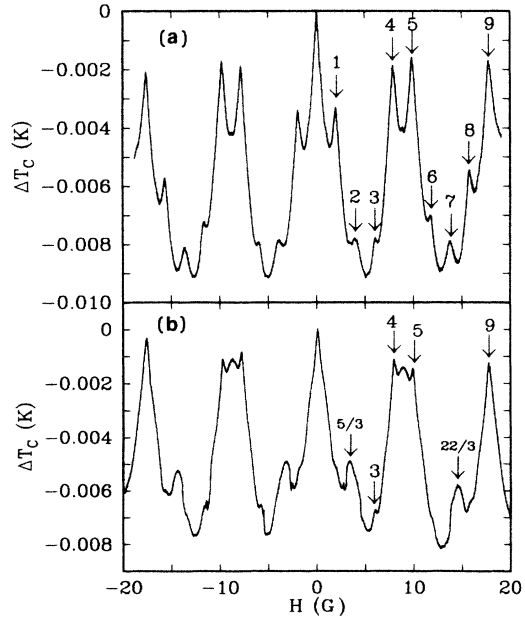

FIG. 2. T_c as a function of external field for the two geometries. The arrows indicate the locations of the maxima corresponding to various n values. (a) $P4gm$. (b) $C2mm$.

It is obvious that for a given n, one can find various sets of (n_{sq},n_{tr}) and we identify the one with the minimum energy as the correct configuration. To help us in this identification, we have done a calculation of the detailed current configurations using the concepts outlined in Ref. 7(b). In particular, we use the London loop condition

$$\sum_l l_{ij}a_{ij}=\frac{2\pi}{a_0}(n_l-\Phi_l/\Phi_0)\,,$$

where a_{ij} is the phase gradient along the strand (ij), l_{ij} is the length of the strand (ij) in units of length a_0, Φ_l is the flux through the loop, and n_l is an integer. An additional condition $\sum_j a_{ij}=0$ at any node i conserves the current. In some cases we had to explicitly impose that the total current across the sample from one end to the other end be zero. The energy required for a given configuration of the currents is then given by

$$\delta U=\tfrac{1}{2}\sum_{(ij)} l_{ij}a_{ij}^2\,.$$

The calculated values of δU (normalized to a basic unit of one square and two triangles) are shown in Table I, by choosing $2\pi/a_0$ to be unity. The depression $\Delta T_c(H)$ from

TABLE I. Identification of the various peaks in Fig. 2. In the cases where we find two sets of (n_{sq},n_{tr}) that are close in δU, for a given lattice and a specific value of n, we give both the configurations. Also, for the same n, the two lattices can have different minimum-energy configurations (n_{sq},n_{tr}), as in the case of $n=10$.

				δU	
n	Φ_{sq}	Φ_{tr}	(n_{sq},n_{tr})	$P4gm$	$C2mm$
$\frac{1}{2}$	0.268	0.116	$(\frac{1}{2},0)$	0.038	0.036
1	0.536	0.232	(1,0)	0.027	0.054
$1\frac{2}{3}$	0.890	0.385	$(1,\frac{1}{3})$	a	b
2	1.072	0.464	$(1,\frac{1}{2})$	0.063	0.052
3	1.608	0.696	(1,1)	0.046	0.093
			$(2,\frac{1}{2})$	0.083	0.089
4	2.144	0.928	(2,1)	0.003	0.005
$4\frac{1}{2}$	2.412	1.044	$(2\frac{1}{2},1)$	0.033	0.024
5	2.680	1.160	(3,1)	0.013	0.026
6	3.215	1.392	$(3,1\frac{1}{2})$	0.069	0.062
7	3.751	1.624	(3,2)	0.072	0.141
			$(4,1\frac{1}{2})$	0.070	0.065
$7\frac{1}{3}$	3.930	1.702	$(4,\frac{5}{3})$	a	b
8	4.287	1.856	(4,2)	0.010	0.020
9	4.823	2.088	(5,2)	0.004	0.008
10	5.359	2.320	$(5,2\frac{1}{2})$	0.079	0.082
			(6,2)	0.052	0.103

[a] Not seen in this geometry.

[b] The lowest-energy solution may involve more than three primitive cells and we have not identified the detailed current configurations to calculate the energy.

the $T_c(0)$ value is proportional to δU.

The limitations of this approach are discussed in Ref. 7(b). In particular, for arbitrary external fields, the current patterns do not have to be commensurate with the underlying lattice and the above approach is not useful. However, for values of n corresponding to an integer or a simple fraction, the minimum periodic unit for the current patterns consists of a small number of the geometrical primitive cell of the lattice under consideration. In these cases, *exact* solutions can be found and they are likely to be the real ground-state configurations.

First, we discuss the $T_c(H)$ of samples of the space group $P4gm$ [Fig. 1(a)]. We have studied three samples of this geometry and found the locations of the structures in T_c to be independent of the details of the lithographic defects in the samples. Relative magnitudes of the various peaks are slightly sensitive to the sample details. In addition, we see evidence to indicate samples of lower resistivity show larger range of coherence as suggested by the observed subharmonic structures. With the help of the calculated values of δU from the detailed current distributions, we confirm the identification of the specific flux configurations. As seen in Table I, the large structures at $n=4$, 5, and 9 result from the fact that for these cases the average values of applied flux (in units of Φ_0) through the square and the triangle (Φ_{sq} and Φ_{tr}, respectively) are both close to integers. In addition to the integer values of n, we find smaller structures at $n=\frac{1}{2}$ and $\frac{9}{2}$.

The numerical solution of the GL equations by Nori and Niu[9] for the $P4gm$ lattice with 400 nodes also shows an excellent agreement with the locations of the experimentally observed maxima. A comparison of the magnitudes of the peaks from Ref. 9 to our δU's requires a scale factor. If the δU for the $n=2$ peak is scaled to match its numerical value from Ref. 9, the δU's for the rest of the peaks agree with their corresponding numerical results to $\simeq \pm 20\%$. This apparent difference between the two calculations may be related to the finite size of the lattice in the numerical calculation. A comparison of the experimental data to either the δU's in Table I or the numerical results of Nori and Niu indicates some discrepancies. For example, the experimental peak at $n=8$ is too small compared to the theoretical predictions. Also, theoretically one expects the peak at $n=4$ to be larger than that at $n=5$, whereas the experimental result is exactly the opposite.

Next, we discuss a sample with the $C2mm$ symmetry. We have studied two samples of this geometry. The detailed current distribution for the $C2mm$ geometry indicates that for many of the flux configurations currents need to flow from one end of the sample to the other, causing the observed structures to be much more sensitive to lithographic defects compared to the $P4gm$ case, where the currents are mostly local. Experimentally, the samples of the $P4gm$ symmetry do yield a cleaner spectrum compared to the $C2mm$ case.

The agreement between the numerical solution[9] for the $C2mm$ lattice with 400 nodes and the δU values in Table I is comparable to the situation for the $P4gm$ case described above. Both calculations predict smaller peaks at $n=1$ and 8, and a larger structure at $n=\frac{9}{2}$ for the $C2mm$ geometry compared to the $P4gm$ case, in agreement with the experiment. Of the two new structures seen in the experiment at $n=\frac{5}{3}$ and $\frac{22}{3}$, the one at $n=\frac{5}{3}$ is predicted by the numerical calculations.[9] Our solution of the detailed current distributions for $n=\frac{5}{3}$ and $\frac{22}{3}$ involving three geometrical primitive cells gives a relatively high value for δU. This implies that the real ground state for these field values may involve more than three primitive cells.

We should emphasize that the theoretical calculations (our London loop equation approach as well as the GL calculations of Ref. 9) assume that the lines defining the network are arbitrarily narrow and the measuring current is zero. Some of the discrepancies between theory and experiment may be ascribed to these assumptions.

Now we discuss the role of irrational ratio of the tile areas in a periodic lattice. This issue has also been addressed by Behrooz *et al.* [see Fig. 9 of Ref. 6(b)]. In contrast with the case of periodic lattice with a single tile, $T_c(H)$ for our networks (after the quadratic subtraction due to the finite width of the wires) is not expected to reach the zero-field value for any nonzero value of the applied field. This is a consequence of the inherent frustration in these lattices due to the fact that the flux quantization cannot be satisfied simultaneously for both the square and the triangle. However, as n_{sq}/n_{tr} approaches a rational approximation to $4/\sqrt{3}$, one sees large structure close to the $T_c(H=0)$ value. It is to be noted from Eq. (1) that the ratio of the numbers of tiles plays a different role in determining the rational or irrational nature of the observed structures compared to the tile-area ratios. In the identification of the peaks in our experiments the tile areas play a role only in determining the basic period and the index n is always rational. This is not the case for the quasiperiodic lattices discussed by Behrooz *et al.*[6]

We have also performed magnetoresistance (MR) measurements just above T_c for both networks. The structures in MR are not as prominent as in $T_c(H)$. The difference between the two lattices is not easy to observe since the major peaks in $T_c(H)$ occur at the same positions. The measurement of the current-voltage characteristics of the networks below T_c also shows a modulation of the critical current in agreement with $T_c(H)$.

In conclusion, we have measured the superconducting-normal phase boundary of periodic networks of two different space-group symmetries that are mixtures of squares and triangles. The networks show maxima in $T_c(H)$ with one major period that averages the areas of the squares and triangles. The magnitudes of the maxima in T_c depend on the exact geometry under consideration.

We thank R. H. Koch for help with the data automation, K. Kwietniak, D. Klaus, and J. Bucchignano for the electron-beam–lithography exposures and processing, C. P. Umbach and J. Kuran for assistance in sample mounting, and R. A. Webb, D. H. Lee, and S. LaPlaca for useful discussions. Especially, we thank F. Nori for sending us the results of numerical calculations prior to publication.

[1]J. M. Kosterlitz and D. J. Thouless, in *Progress in Low Temperature Physics,* edited by D. F. Brewer (North-Holland, Amsterdam, 1978), Vol. VIIB, p. 371.

[2]R. A. Webb, R. F. Voss, G. Grinstein, and P. M. Horn, Phys. Rev. Lett. **51**, 690 (1983); B. J. van Wees, H. S. J. van der Zant, and J. E. Mooij, Phys. Rev. B **35**, 7291 (1987).

[3]C. J. Lobb, Physica B+C **126B**, 319 (1984).

[4]B. Pannetier, J. Chaussy, R. Rammal, and J. C. Villegier, Phys. Rev. Lett. **53**, 1845 (1984); B. Pannetier, J. Chaussy, and R. Rammal, J. Phys. (Paris) Lett. **44**, L853 (1983).

[5]J. M. Gordon, A. M. Goldman, J. Maps, D. Costello, R. Tiberio, and B. Whitehead, Phys. Rev. Lett. **56**, 2280 (1986); J. M. Gordon and A. M. Goldman, Phys. Rev. B **35**, 4909 (1987).

[6](a) A. Behrooz, M. J. Burns, H. Deckman, D. Levine, B. Whitehead, and P. M. Chaikin, Phys. Rev. Lett. **57**, 368 (1986); (b) A. Behrooz, M. J. Burns, D. Levine, B. Whitehead, and P. M. Chaikin, Phys. Rev. B **35**, 8396 (1987).

[7](a) S. Alexander, Phys. Rev. B **27**, 1541 (1983); (b) S. Alexander and E. Halevi, J. Phys. (Paris) **44**, 805 (1983).

[8]R. Rammal, T. C. Lubensky, and G. Toulouse, Phys. Rev. B **27**, 2820 (1983).

[9]F. Nori and Q. Niu, the following paper, Phys. Rev. B **37**, 2364 (1988).

[10]W. W. Molzen, P. D. Gerber, A. M. Schweighart, M. R. Wordeman, R. G. Viswanathan, and A. D. Wilson, in *Proceedings of Microcircuit Engineering '84,* edited by A. Heuberger and H. Beneking (Academic, London, 1985), p. 219.

[11]*International Tables for X-Ray Crystallography* (Kynoch, Birmingham, 1952), Vol. 1.

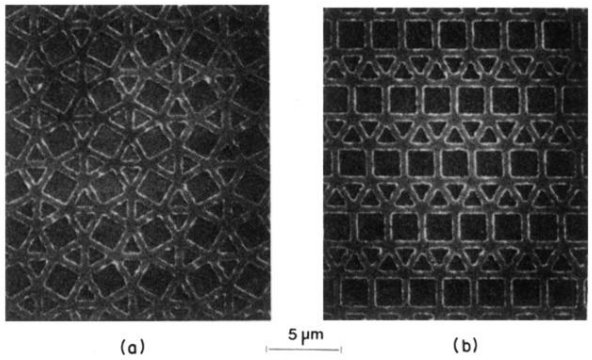

FIG. 1. Electron micrographs of samples. (a) $P4gm$ symmetry. (b) $C2mm$ symmetry.